A Joint MAC and Physical Layer Analytical Model for IEEE 802.11a Networks Operating under RTS/CTS Access Scheme

Roger Pierre Fabris Hoefel

Department of Telecommunications Engineering - University La Salle
92010-000 - Canoas - RS - Brazil

roger@lasalle.tche.br

Abstract. *It is proposed an analytical cross-layer saturation goodput model for the IEEE 802.11a physical (PHY) and medium access control (MAC) layers. It is assumed an ad hoc network operating under the distributed coordination function (DCF) using the request-to-send/clear-to-send (RTS/CTS) operational mode. The proposed analytical expressions, which are validated by simulation, allow assessing the effects on the system performance of channel load, contention window resolution algorithm, distinct modulation schemes, forward error corrector (FEC) coding schemes, receivers structures and channel models.*

Resumo. *Neste artigo é proposto um modelo teórico que permite analisar de maneira integrada o desempenho das camadas de enlace e física de redes locais sem fio IEEE 802.11a. As expressões analíticas propostas permitem verificar os efeitos no desempenho do sistema da carga no canal, do algoritmo de resolução da janela de contenção, de esquemas de modulação, integrados com códigos corretores de erro, das estruturas do receptor e de modelos de canal.*

1. Introduction

In [BIANCHI 2000], it is carried out a theoretical analysis of the IEEE 802.11 DCF MAC protocol in the assumption of ideal channel conditions. In [QIAO 2002], considering a network loaded with two stations (STAs) that generate deterministic traffic, it is developed an analytical model to jointly evaluate the performance of IEEE 802.11a MAC and PHY layer protocols. In [HOEFEL 2004], we developed a theoretical cross-layer model for MAC and PHY layer protocols for networks based on the IEEE 802.11 family of specifications. The analytical expressions derived allow estimate the effects of distinct modulation schemes, channel models and an adaptive link level scheme on the system performance. However, in [HOEFEL 2004] the MAC 802.11 contention window (CW) resolution was not implemented (i.e. the packets are dropped after the first non-successful transmission attempted) in order that the simulated offered traffic follows strictly the Poisson statistics, as analytically postulated. In this contribution, we use the methodology proposed by Bianchi in [BIANCHI 2000] in order to develop a theoretical cross-layer goodput analysis for IEEE 802.11a networks. The proposed model takes into account the effects of *backoff scheme* and *non-ideal channel*

conditions (i.e. MAC and PHY layer issues). Simulation results, obtained using a joint C^{++} IEEE 802.11 system level and link level simulator, are used in order to validate the proposed theoretical model. This paper is divided as follows. Section 2 presents a brief description of the IEEE 802.11 DCF medium MAC protocol. The development of analytical expressions for the net saturation throughput (or goodput) is done at Section 3. Section 4 presents a comparison between numerical and simulation results, while the final remarks are drawn in Section 5.

2. The IEEE 802.11 DCF RTS/CTS access scheme

The DCF implements the Carrier Sense Multiple Access with Collision Avoidance (CSMA/CA) protocol [IEEE 802.11 1999], i.e. a mandatory random access protocol where physical and virtual carrier sensing functions indicates if the channel is busy or idle. The virtual carrier sensing is implemented using the network allocation vector (NAV). This timer, which is updated by a control field transmitted in data and control frames, sets the amount of time the channel is reserved to provide uninterrupted atomic transmissions. The DCF can be used on Infrastructure Base Service Set (IBSS) networks, where access points (APs) and wired backbones are implemented, and on Independent BSS (or ad hoc) networks, where communication is done at peer-to-peer basis. The DCF has the following distributed access polices [IEEE 802.11 1999]: *(1)* basic positive acknowledgment (ACK); *(2)* RTS/CTS clearing technique. In this paper, we only analyze the second one due to space constraints.

Fig. 1 shows the clearing technique used at atomic RTS/CTS operational mode. The station 1 (STA1) only accesses the channel after implementing the physical carrier-sensing and virtual carrier-sensing functions. If the channel is idle, then the transmission of a RTS control frame can begin immediately, as long as the channel remains idle for a time longer than the DCF interframe spacing (DIFS). If the channel is busy, the STA1 must backoff its transmission until the channel becomes idle for the DIFS period. After this DIFS period: *(1)* it starts to treat the channel in units of time slot; *(2)* it implements a binary exponential backoff period (EBP) to determine the access time in time slots; *(3)* it keeps checking the channel to verify if it is busy or idle. The STA1 decrements the EBP while the channel is idle. If the channel is busy, the decrement of backoff interval stops and it only resumes after the channel is detected idle for a DIFS period. If the channel remains idle when the EBP becomes zero, then the STA1 transmits a RTS control frame. If the RTS frame transmission is successful, the peer station (STA2) sends a CTS control frame to confirm the reservation. After that, it is transmitted a MAC protocol data unit (MPDU) unicast frame. If the MPDU transmission is successful, then the peer station must transmit an ACK control frame after a short interframe spacing (SIFS) period. The sender STA must use the extended interframe spacing (EIFS) to set the time for new physical channel sensing if either data or control frames are corrupted or due to the timeout of timer that controls the maximum expected delay. It is again used a binary EBP to set the time slot, but now the CW is doubled at each unsuccessful transmission. The CW is reset after a successful transmission. The data frame is dropped after a given number of transmission attempts.

3. Analytical results for the net saturation throughput

Fig. 2 shows a discrete bi-dimensional Markov chain *(s(t),b(t))* for the backoff window size assuming the RTS/CTS scheme with positive ACK of data, where *s(t)* is the

stochastic process of the backoff stage *(0, ···,m)* of the STA at time *t* and *b(t)* is the random process that models the backoff time counter for a given STA. This model assumes that each packet collides with a constant and independent *conditional collision probability p.* It is also assumed a fixed number of *n* STAs operating in saturation conditions, i.e. each STA has a packet to transmit after the completion of each successful transmission.

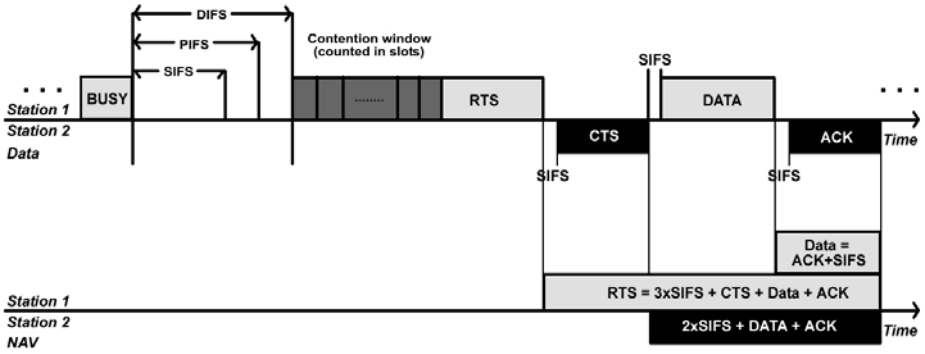

Figure 1. The clearing technique used at atomic RTS/CTS scheme.

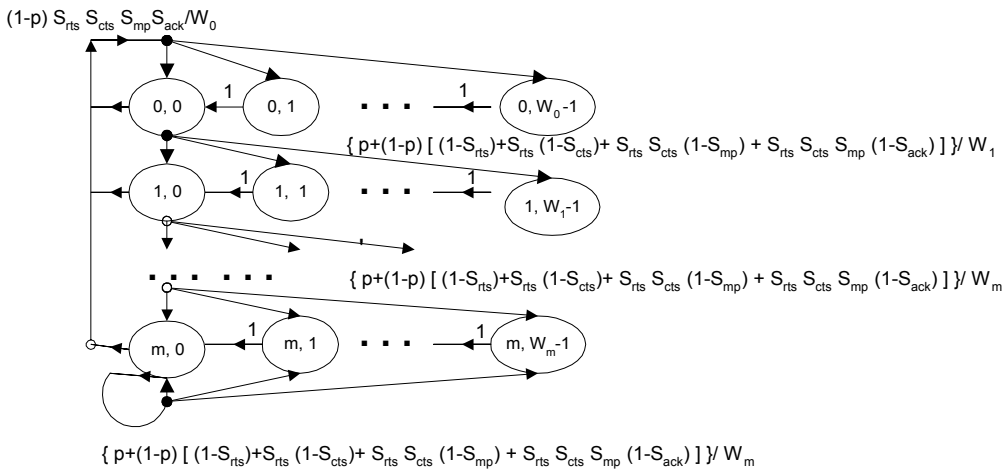

Figure 2. Bi-dimensional Markov chain *(s(t),b(t))* model for the backoff window size and a non-ideal channel.

3.1 Packet Transmission Probability

Using the short notation $P\{i_1,k_1/i_0,k_o\}=P\{s(t+1)=i_1,b(t+1)=k_1|s(t)=i_o,b(t)=k_o\}$, equations (1) to (4) model the null one-step transition probabilities of the Markov chain depicted at Fig. 2.

$$P\{i,k \mid i,k+1\}=1 \quad for\ \ k\in(0,W_i-2)\ \ and\ \ i\in(0,m). \tag{1}$$

$$P\{0,k \mid i,0\}=(1-p)S_{rts}S_{cts}S_{mp}S_{ack}/W_0 \quad for\ \ k\in(0,W_0-1)\ and\ \ i\in(0,m) \tag{2}$$

$$P\{i,k \mid i-1,0\} = \{p + (1-p)[(1-S_{rts}) + S_{rts}(1-S_{cts}) + S_{rts}S_{cts}(1-S_{mp}) + S_{rts}S_{cts}S_{mp}(1-S_{ack})]\}/W_i$$

$k \in (0,W_i\text{-}1)$ and $i \in (1,m)$. (3)

$$P\{m,k \mid m,0\} = \{p + (1-p)[(1-S_{rts}) + S_{rts}(1-S_{cts}) + S_{rts}S_{cts}(1-S_{mp}) + S_{rts}S_{cts}S_{mp}(1-S_{ack})]\}/W_m$$

$k \in (0,W_m\text{-}1)$. (4)

The window size at backoff stage i is labeled as $W_i = 2^i W$, where $i \in (0,m)$ is the backoff stage and W is the MAC CW size parameter CW_{min} The maximum window size is denoted as $W_m = 2^m W - 1 = CW_{max} - 1$.

Eq. (1) models the decreasing of the backoff timer at the beginning at each slot time of size σ.

Eq. (2) takes into account that a new physical layer convergence procedure (PCLP) protocol data unit (PPDU) starts at backoff stage 0 and that the backoff is uniformly distributed into the range $(0, W_0\text{-}1)$ after a successful PPDU transmission. S_{cts}, S_{rts} and S_{ack} denote, respectively, the probability that the RTS, CTS and ACK control frames be transmitted with success. S_{mp} denotes the probability that the transmission of a MPDU (i.e. a MAC PDU) is successful.

Eq. (3) models the fact that a new backoff value is uniformly chosen in the range $(0,W_i)$ after an unsuccessful transmission at the backoff stage $i\text{-}1$. The capture effect is neglected in such way that the lost of frames due to collisions is independent of the lost of frames due to noise and interference.

Eq. (4) models the fact that the backoff is not increased in subsequent frame transmissions once the backoff stage has reached the value m.

The closed-form solution for the stationary distribution for this Markov chain can be obtained as follows.

For $0 < i < m$, we have that

$$b_{i\text{-}1,0} \cdot \left\{ p + (1-p) \cdot \begin{bmatrix} (1 - S_{rts}) + S_{rts}(1 - S_{cts}) + S_{rts}S_{cts}(1 - S_{mp}) + \\ S_{rts}S_{cts}S_{mp}(1 - S_{ack}) \end{bmatrix} \right\} = b_{i,0}, \quad (5a)$$

$$b_{i\text{-}1,0} \cdot \{p + (1-p) \cdot [\ 1 - S_{rts}S_{cts}S_{mp}S_{ack}\ ]\} = b_{i,0}, \quad (5b)$$

$$b_{i,0} = \left[1 + S_{rts}S_{cts}S_{mp}S_{ack}(p-1)\right]^i b_{0,0}\ . \quad (5c)$$

We also have that

$$[b_{m-1,0} + b_{m,0}] \cdot \left\{ p + (1-p) \cdot \begin{bmatrix} (1 - S_{rts}) + S_{rts}(1 - S_{cts}) + S_{rts}S_{cts}(1 - S_{mp}) + \\ S_{rts}S_{cts}S_{mp}(1 - S_{ack}) \end{bmatrix} \right\} = b_{m,0}, \quad (6a)$$

$$[b_{m-1,0} + b_{m,0}] \cdot \{p + (1-p) \cdot [1 - S_{rts}S_{cts}S_{mp}S_{ack}]\} = b_{m,0}, \quad (6b)$$

$$b_{m,0} = \frac{\left[1 + S_{rts}\ S_{cts}\ S_{mp} S_{ack}\,(p-1)\right]^m}{(1-p)\,S_{cts}\ S_{rts}\ S_{mp}\ S_{ack}}\, b_{0,0}\,, \tag{6c}$$

where it is used (5c) in (6b) for $m=i$.

Due to the Markov chain regularities, for each $k \in (0, W_m\text{-}1)$, we have that

$$b_{i,k} = \frac{W_i - k}{W_i} \cdot \begin{cases} (1-p)\cdot S_{rts}\cdot S_{cts}\cdot S_{mp}\cdot S_{ack} \sum_{j=0}^{m} b_{j,0} & for \quad i = 0 \\ b_{i\text{-}1,0}\left[\, p + (1-p)\left(1 - S_{rts} S_{rts} S_{mp} S_{ack}\right)\,\right] & for \quad 0 < i < m \\ \left[\, p + (1-p)\left(1 - S_{rts} S_{rts} S_{mp} S_{ack}\right)\,\right]\left(b_{m\text{-}1,0} + b_{m,0}\right) & for \quad i = m \end{cases} \tag{7}$$

Using (5b) and (6b), then (7) can be rewritten as

$$b_{i,k} = \frac{W_i - k}{W_i} \cdot b_{i,0}\,, \tag{8}$$

since (see 5c and 6c)

$$\begin{aligned} \sum_{i=0}^{m} b_{i,0} &= \sum_{i=0}^{m-1} \left[1 + S_{rts}\ S_{cts}\ S_{mp}\ S_{ack}\ (p-1)\right]^i b_{0,0} + b_{m,0} \\ &= \frac{b_{0,0}}{S_{rts}\ S_{cts}\ S_{mp} S_{ack}\,(1-p)} \end{aligned} \tag{9}$$

We can impose the following normalization condition:

$$1 = \sum_{i=0}^{m} \sum_{k=0}^{W_i - 1} b_{i,k} = \sum_{i=0}^{m} b_{i,0} \sum_{k=0}^{W_i - 1} \frac{W_i - k}{W_i} = \sum_{i=0}^{m} b_{i,0}\, \frac{W_i + 1}{2} = \sum_{i=0}^{m} b_{i,0}\, \frac{2^i W + 1}{2}\,. \tag{10}$$

Using (5c), (6c) and (9), then (10) can be simplified to

$$1 = \frac{b_{0,0}}{2} \left\{ W \left[\begin{array}{l} \sum_{i=0}^{m-1} 2^i \left[1 + S_{rts}\, S_{cts}\, S_{mp} S_{ack} (p-1)\right]^i + \\ 2^m \dfrac{\left[1 + S_{rts}\, S_{cts}\, S_{mp}\, S_{ack} (p-1)\right]^m}{(1-p)\, S_{rts}\, S_{cts}\, S_{mp}\, S_{ack}} \end{array} \right] + \frac{1}{S_{rts}\, S_{cts}\, S_{mp}\, S_{ack} (1-p)} \right\}. \tag{11}$$

Using $S = S_{rts}\, S_{cts}\, S_{mp}.\, S_{ack}$, we can show that

$$b_{0,0} = \frac{2(1-p)\cdot S \cdot \left[1 + 2\cdot S\cdot (p-1)\right]}{1 + 2^m W \cdot \left[1 + (-1+p)\cdot S\right]^m + (-1+p)\cdot S \cdot \left\{2 + W + 2^m W \cdot \left[1 + (-1+p)\cdot S\right]^m\right\}} \tag{12}$$

Notice that for an ideal channel (i.e. $S_{rts} = S_{cts} = S_{mp} = S_{ack} = 1$), Eq. (12) resumes to

$$b_{0,0} = \frac{2\cdot (1-2p)\cdot (1-p)}{(1-2p)\cdot (W+1) + pW \cdot \left[1 - (2p)^m\right]}, \tag{13}$$

which is in agreement with Eq (6) of [BIANCHI 2000].

Any transmission occurs when the backoff timer counter is equal to zero, then the probability that a STA transmits in a randomly chosen slot time is (see 9)

$$\tau = \sum_{i=0}^{m} b_{i,0} = \frac{b_{0,0}}{S \cdot (1-p)} = \frac{b_{0,0}}{S_{rts} \cdot S_{cts} \cdot S_{mp} \cdot S_{ack} \cdot (1-p)}. \quad (14)$$

When there is no exponential backoff, then using (13) with $m=0$, we have that

$$\tau = \frac{2}{W+1}, \quad (15)$$

in according with Eq. (8) of [BIANCHI 2000].

Each STA transmits with probability τ. Therefore, the probability that a transmitted PPDU encounters a collision in a given slot time can be stated as

$$p = 1-(1-\tau)^{n-1}, \quad (16)$$

The nonlinear system represented by (14) and (16) can be solved using numerical techniques.

3.2 Goodput

The net throughput in *bits per second (bps)* can be stated as the probability that a MAC payload with N_{pl} *octets* be transmitted with success in the average cycle time $\overline{T}$, i.e.

$$G_{bps} = \frac{8 \cdot N_{pl} \cdot P_s \cdot P_{tr} \cdot S_{rts} \cdot S_{cts} \cdot S_{mp} \cdot S_{ack}}{\overline{T}}. \quad (17)$$

The probability that there is no collision on the channel conditioned to the fact that at least one STA transmits is given by

$$P_s = \frac{\binom{n}{1} \cdot \tau \cdot (1-\tau)^{n-1}}{P_{tr}} = \frac{n \cdot \tau \cdot (1-\tau)^{n-1}}{P_{tr}} = \frac{n \cdot \tau \cdot (1-\tau)^{n-1}}{1-(1-\tau)^{n}}, \quad (18)$$

where P_{tr} is the probability that there is at least one transmission in the considered slot time. Notice that it is assumed in (17) and (19) that the lost of frames due to collisions is independent of the lost of frames due to noise.

The average cycle time is given by

$$\overline{T} = \overline{B}_s + \overline{B}_{f1} + \overline{B}_{f2} + \overline{B}_{f3} + B_{f4} + B_{f5} + \bar{I}, \quad (19)$$

The average busy time when the transmission is successful is given by:

$$\overline{B}_s = P_s \cdot P_{tr} \cdot S_{rts} \cdot S_{cts} \cdot S_{mp} \cdot S_{ack} \cdot \left[DIFS + T_{rts}(p_{rts}) + a + SIFS + T_{cts}(p_{cts}) + a + SIFS + T_{mp}(p_{mp}) + a + SIFS + T_{ack}(p_{ack}) + a\right], \quad (20)$$

where a is the propagation delay. $T_{rts}(p_{rts})$, $T_{cts}(p_{cts})$ and $T_{ack}(p_{ack})$ denote the time necessary to transmit the RTS, CTS and ACK control frames when it is used the *PHY mode* p_{rts}, p_{cts} and p_{ack}, respectively. $T_{mp}(p_{mp})$ is the time necessary to transmit a MPDU payload when it is used the *PHY mode* m_{mp}.

$\overline{B}_{f1}$, models the average amount of time in which the channel is busy due to collisions at the transmission of RTS control frames, whereas $\overline{B}_{f2}$, $\overline{B}_{f3}$, $\overline{B}_{f4}$ and $\overline{B}_{f5}$ model the average time that the channel is busy with unsuccessful transmissions, due to noise and interference, of RTS, CTS, data and ACK frames, respectively.

$$\overline{B}_{f1} = P_{tr} \cdot (1 - P_s) \cdot \left[EIFS + T_{rts}(p_{rts}) + a \right]. \tag{21}$$

$$\overline{B}_{f2} = P_{tr} \cdot P_s \cdot (1 - S_{rts}) \left[EIFS + T_{rts}(p_{rts}) + a \right]. \tag{22}$$

$$\overline{B}_{f3} = P_{tr} \cdot P_s \cdot S_{rts} \cdot (1 - S_{cts}) \left[EIFS + T_{rts}(p_{rts}) + a + SIFS + T_{cts}(p_{cts}) + a \right]. \tag{23}$$

$$\begin{aligned} \overline{B}_{f4} = P_{tr} \cdot P_s \cdot S_{rts} \cdot S_{cts} \cdot (1 - S_{mp}) \left[EIFS + T_{rts}(p_{rts}) + \right. \\ \left. a + SIFS + T_{cts}(p_{cts}) + a + SIFS + T_{mp}(p_{mp}) + a \right]. \end{aligned} \tag{24}$$

$$\begin{aligned} \overline{B}_{f5} = P_{tr} \cdot P_s \cdot S_{rts} \cdot S_{mp} \cdot (1 - S_{ack}) \left[EIFS + T_{rts}(p_{rts}) + \right. \\ a + SIFS + T_{rcs}(p_{cts}) + a + SIFS + T_{mp}(p_{mp}) + a + \\ \left. SIFS + T_{ack}(p_{ack}) + a \right]. \end{aligned} \tag{25}$$

where a is the propagation delay, T_{mp} is the time necessary to transmit a MAC PDU, DIFS is the DCF interframe spacing (IFS), SIFS is the short IFS and EIFS is the extended IFS.

The average time that a slot time is idle is given by

$$\overline{I} = (1 - P_{tr}) \cdot \sigma \ . \tag{26}$$

For an ideal channel (i.e. S_{rts}=S_{cts}= S_{mp}= S_{ack} =*1*), (17) resumes

$$G = \frac{8 \cdot N_{pl} \cdot P_s \cdot P_{tr}}{\overline{B}_s + \overline{B}_{f1} + \overline{I}}, \tag{27}$$

in according with (13) of [BIANCHI 2000].

3.3 Frame Success Probability for 802.11a

The IEEE 802.11a is based on Orthogonal Frequency Division Modulation (OFDM) using a total of 52 subcarriers, of which 48 subcarriers carry actual data and four subcarriers are pilots used to facilitate coherent detection [IEEE 802.11a 1999]. The OFDM symbol interval, *tSymbol*, is set to 4μs. Therefore, the channel symbol rate R_s is of *12 Msymbols/sec*.

Tab. 1 shows the OFDM PHY characteristics, where *BpS* means Bytes per Symbol. For instance, the *PHY mode 1* carries 3 bytes per symbol, i.e. 6 Mbps* *tSymbol/8.0=3 BpS.*

The convolutional encoders use the industry-standard generator polynomials, $\boldsymbol{g_0}=(133)_8$ and $\boldsymbol{g_1}=(171)_8$, of rate *r=1/2* and constraint length *K=7* [IEEE 802.11a 1999]. The transfer function, using the data tabulated in [CONAN 1984], is given by (28).

Tab. 1. The IEEE 802.11a PHY modes.

Mode m	*Modulation*	*Code Rate R_c*	*Data Rate*	*BpS*
1	BPSK	1/2	6 Mbps	3
2	BPSK	3/4	9 Mbps	4.5
3	QPSK	1/2	12 Mbps	6
4	QPSK	3/4	18 Mbps	9
5	16-QAM	1/2	24 Mbps	12
6	16-QAM	3/4	36 Mbps	18
7	64-QAM	2/3	48 Mbps	24
8	64-QAM	3/4	54 Mbps	27

$$T_{1/2}(D) = 11D^{10} + 38D^{12} + 193D^{14} + 1331D^{16} + 7275D^{18} + 40406D^{20} + 234969D^{22} + \cdots . \quad (28)$$

The higher code rates of 2/3 and 3/4 are obtained by puncturing the original rate-1/2 code [IEEE 802.11a 1999]. The transfer function, using the data tabulated in [Haccoun 1999], for the code rate 2/3 is given by (29), whereas the transfer function for the code rate 3/4 is given by (30).

$$T_{2/3}(D) = D^6 + 16D^7 + 48D^8 + 158D^9 + 642D^{10} + 2435D^{11} + 9174D^{12} + 34705\ D^{13} + \cdots . \quad (29)$$

$$T_{3/4}(D) = 8D^5 + 31D^6 + 160D^7 + 892D^8 + 4512D^9 + 23307D^{10} + 121077D^{11} + 625059D^{12} + \cdots . \quad (30)$$

Fig. 3 shows the PLCP Protocol Data Unit (PPDU) of the IEEE 802.11a: *(1)* the PLCP preamble duration, *tPCLPPreamble*, is equal to 12 μs; (2*)* the PCLP field duration, *tPCLP_SIG*, is equal to *4 μs*. Both MPDU frames and RTS, CTS and ACK control frames are encapsulated in the PPDU as shown at Fig. 3.

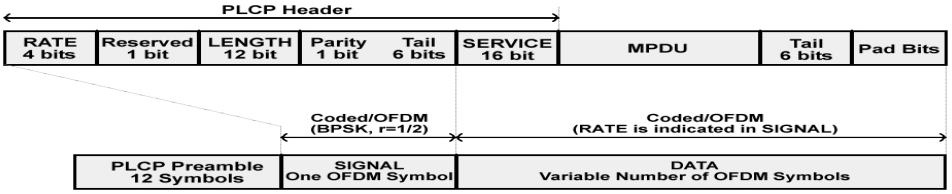

Figure 3. PPDU frame format of the IEEE 802.11a [IEEE 1999b].

The RTS and CTS control frames must be transmitted at one of the rates of the basic service set (BSS) so that they can be decoded by all the STSs in the same network. The mandatory BSS basic rate set is {6 Mbps, 12 Mbps, 24 Mbps}. The ACK control frame must be transmitted using the BSS basic rate that is less than or equal to the rate of the data frame it is acknowledging.

As shown at Fig. 3, that the *SERVICE* field has 16 bits and that 6 tail bits are used to flush the convolutional code to the "zero state". Therefore, the duration of RTS and CTS frames are given by (31) and (32), respectively. The RTS and CTS have l_{rts}*=20 bytes* and l_{cts}*=14 bytes*, respectively [IEEE 802.11a 1999].

$$T_{rts}(m_{rts}) = tPCLPPreamble + tPCLP\_SIG + \left\lceil \frac{l_{rts} + (16+6)/8}{BpS(p_{rts})} \right\rceil tSymbol\ . \quad (31)$$

$$T_{cts}(m_{cts}) = tPCLPPreamble + tPCLP\_SIG + \left\lceil \frac{l_{cts} + (16+6)/8}{BpS(p_{cts})} \right\rceil tSymbol\ . \quad (32)$$

The transmission period to transmit a MPDU with a payload of *l octets* over the IEEE 802.11a using the *PHY mode m* is given by (33). The MPDU header and the cyclic redundant checking (CRC) fields have together a length of 34 bytes [IEEE 802.11 1999, pp. 52]. The ACK transmission time, whose length is of l_{ack}*=14 bytes* [IEEE 802.11 1999, pp. 64], is given by (34) assuming the *PHY mode* m_{ack}.

$$T_{mp}(m) = tPCLPPreamble + tPCLP\_SIG + \left\lceil \frac{l + 34 + (16+6)/8}{BpS(p_{mp})} \right\rceil tSymbol\ . \quad (33)$$

$$T_{ack}(m_{ack}) = tPCLPPreamble + tPCLP\_SIG + \left\lceil \frac{l_{ack} + (16+6)/8}{BpS(p_{ack})} \right\rceil tSymbol\ . \quad (34)$$

Assuming that the convolutional forward error correcting code (FEC) is decoded using hard-decision Viterbi decoding, then (35) and (36) model the probability of incorrectly selecting a path when the Hamming distance *d* is even and odd, repesctivly. The used notation emphasizes the dependence of P_d with the received signal-to-interference-plus-noise (SINR) per bit γ_b, and the *PHY mode p* [QIAO 2002]. The bit error rate (BER) for the *PHY mode m* modulation scheme is denoted by ρ_m.

$$P_d(\gamma_b, \rho_m) = \frac{1}{2}\binom{d}{d/2}\rho_m^{d/2}(1-\rho_m)^{d/2} + \sum_{k=d/2+1}^{d}\binom{d}{k}\rho_m^k(1-\rho_m)^{d-k}. \quad (35)$$

$$P_d(\gamma_b, \rho_m) = \sum_{k=(d+1)/2}^{d}\binom{d}{k}\rho_m^k(1-\rho_m)^{d-k}. \quad (36)$$

Considering the IEEE 802.11a generator polynomials, $\boldsymbol{g_0}=(133)_8$ and $\boldsymbol{g_1}=(171)_8$, of rate *r=1/2* and constrain length *K=7* [IEEE 802.11 1999, pp.16] and using (28), then the union bound on the probability of decoding error is given by (37). Correspondingly, using (29) and (30), then the union bound on the probability of decoding error for the code rates 2/3 and 3/4 are given by (38) and (39), respectively.

$$P_e(\gamma_b, \rho_m) < 11\,P_{10}(\gamma_b, \rho_m) + 38\,P_{12}(\gamma_b, \rho_m) + 193\,P_{14}(\gamma_b, \rho_m) + \cdots. \quad (37)$$

$$P_e(\gamma_b, \rho_m) < P_6(\gamma_b, \rho_m) + 16\,P_7(\gamma_b, \rho_m) + 48\,P_8(\gamma_b, \rho_m) + \cdots. \quad (38)$$

$$P_e(\gamma_b, \rho_m) < 8P_5(\gamma_b, \rho_m) + 31\,P_6(\gamma_b, \rho_m) + 160\,P_7(\gamma_b, \rho_m) + \cdots. \quad (39)$$

Postulating that the errors inside of the decoder are interdependent, then *Pursley* and *Taipale* have shown that the upper bound for a successful transmission of a frame with *l* octets is given by [PURSLEY 1987]

$$S(l,\gamma_b,\rho_m) < \left[1 - P_e(\gamma_b,\rho_m)\right]^{8l}. \quad (40)$$

3.4 Bit Error Rate (BER) for Uncorrelated Fading Channel

It is assumed a Rayleigh fading temporally independent at symbol level and independent across of the OFDM carriers.

Using the uncorrelated channel assumption and considering that the PCLP header with 24 bits is always transmitted using PHY mode 1 (see Fig. 3). Then, the successful MPDU transmission is given by

$$S_{mp}(l,\gamma_b,\rho_m) = S(24/8,\gamma_b,1)\, S(34+(16+6)/8+N_{pl},\gamma_b,\rho_m), \quad (41)$$

where the MPDU header and the CRC fields have together a length of 34 bytes, the SERVICE field has 16 bits and 6 bits are used to set the convolutional coder to the zero state. Correspondingly, the RTS, CTS and ACK control frames success probabilities are given by (42), (43) and (44), respectively.

$$S_{rts}(l,\gamma_b,\rho_{rts}) = S(24/8,\gamma_b,1)\, S(20+(16+6)/8,\gamma_b,\rho_{rts}). \quad (42)$$

$$S_{cts}(l,\gamma_b,\rho_{cts}) = S(24/8,\gamma_b,1)\, S(14+(16+6)/8,\gamma_b,\rho_{cts}). \quad (43)$$

$$S_{ack}(l,\gamma_b,\rho_{ack}) = S(24/8,\gamma_b,1)\, S(14+(16+6)/8,\gamma_b,\rho_{ack}). \quad (44)$$

Considering a maximum ratio combining (MRC) receiver matched with the channel diversity and that the same average power Ω is received at each diversity branch, then the probability distribution function (pdf) of the SINR per bit at the receiver is of gamma kind [HOEFEL 1999], i.e.

$$p(\gamma_b) = \frac{1}{\Gamma(L)}\left(\frac{1}{\bar{\gamma}_b}\right)^L (\gamma_b)^{L-1} \exp\left(-\frac{\gamma_b}{\bar{\gamma}_b}\right) \quad if\ \ \gamma_b > 0, \quad (45)$$

where Γ is the gamma function, $\bar{\gamma}_b$ is the average SINR per bit at the receiver output and *L* is the number of diversity branches.

The average BER for BPSK and QPSK signaling is given [PROAKIS 2001]

$$\overline{P_e} = \rho = \int_0^\infty Q\left(\sqrt{2\,R_c\gamma_b}\right) p(\gamma_b)\, d\gamma_b, \quad (46)$$

where *Q(x)* is the complementary Gaussian cumulative distribution function and R_c is the code rate.

The average BER for M-QAM signaling is given by [Yang 2000]

$$\overline{P_e} = \rho = \frac{\sqrt{M}-1}{\sqrt{M}\log_2\sqrt{M}} \int_0^{\infty} erfc\left(\sqrt{\frac{2\log_2 M \cdot R_c \cdot \gamma_b}{2(M-1)}}\right) p(\gamma_b) d\gamma_b + \frac{\sqrt{M}-2}{\sqrt{M}\log_2\sqrt{M}} \int_0^{\infty} erfc\left(\sqrt{\frac{3\log_2 M \cdot R_c \cdot \gamma_b}{2(M-1)}}\right) p(\gamma_b) d\gamma_b, \quad (47)$$

where *erfc(z)* is the complementary error function.

4. Model Validation

The C^{++} IEEE 802.11a MAC and PHY layer simulator (i.e. an integrated system level and link level simulator) implemented in this paper has the following main characteristics:

- It is assumed an ad-hoc network, as such as the DCF MAC protocol is used.
- It is implemented the MAC state machine that fulfills the RTS/CTS clearing technique (Fig. 1) specified at the IEEE 802.11 management information base (MIB).
- The OFDM PHY layer is implemented assuming perfect synchronism. The physical layer signal processing algorithms implements the maximum-likelihood hard decision detection for the PHY mode 1 to PHY 8.
- The convolutional hard-decision decoding is constructed using a semi-analytic approach as follows. The average BER is estimated at a frame basis using on-line statistics collected at the demodulator output. Then the average BER is used in (40) to estimate the probability of the successful MPDU transmission. The used modular software design permits that the Viterbi convolutional decoding can be implemented as a plug-in function. This methodology, besides speeding-up the computational time, offers powerful insights on the system performance as well as on the fundamental issue of software validation.
- It is assumed the following parameters: *slot time* σ*=9*μ*S, SIFS=16* μ*s, DIFS=EIFS=34* μ*s,* CW_{min}*=16,* CW_{max}*=1023, m=6, a=1*μ*.s,* N_{pl}*=1023 octets.*

Fig. 4 shows a good agreement between numerical and simulation results when the system is lightly (10 STAs) and heavily (30 STAs) loaded. Here, it is assumed that all STAs are transmitting using the PHY mode 1. Fig. 4 also shows the goodput does not change significantly when the number of STAs is increased from 10 to 30. This occurs because the increase of collisions, besides to be restricted to the short lenght RTS control frames, is counterbalanced by the diminishing of the average idle time (see 26) when the channel load is increased.

Fig. 5 shows again a good agreement between numerical and simulation results for the BSS PHY modes. It is noticed, as theoretically expected, that the net effect of increasing the number of received antennas on the system performance follows the law of decreasing gains.

Fig. 6a compares the goodput as a function of the SINR per bit for a system without spatial diversity. Fig. 6a permit to drawn some interesting remarks on the effects of SINR per bit on the system performance. First, we can verify that the *PHY mode 3* (QPSK with R_c=1/2) allows a superior performance in relation to that one obtained with the *PHY mode 1* (BPSK with R_c=1/2) since the QPSK signalling has a better spectral efficiency when it is implemented coherent demodulation. Notice that this also explains the better performance of *PHY mode 4* (QPSK with R_c=3/4) in relation to the *PHY mode*

2 (BPSK with R_c=3/4) signalling scheme. Second, *PHY mode 5* (16QAM with R_c=1/2) has a better performance than the *PHY mode 2* (BPSK with R_c=3/4) and *PHY mode* 4 (QPSK with R_c=3/4). This interesting characteristic occurs due to the high coding gain allowed in environments where the Rayleigh multipath fading is temporally independent at symbol level (see 45, 46 and 47), as postulated in this contribution. Third, *PHY mode 7* (64QAM with R_c=2/3) has a better performance in relation to the *PHY mode 6* (16QAM with R_c=3/4) since the higher coding gain overwhelm (in the assumed channel model) the greater noise immunity of 16QAM in relation to the 64QAM signalling scheme. Finally, Fig. 6b shows that when the net effect of the fading is less severe due to spatial diversity, then we can determine (differently of observed at Fig. 6a) a range of γ_b where the performance of *PHY mode 4* is superior in relation to the performance obtained with the *PHY mode 5* and a region where the performance of *PHY mode 6* superior in relation to the performance observed with the *PHY mode 7*.

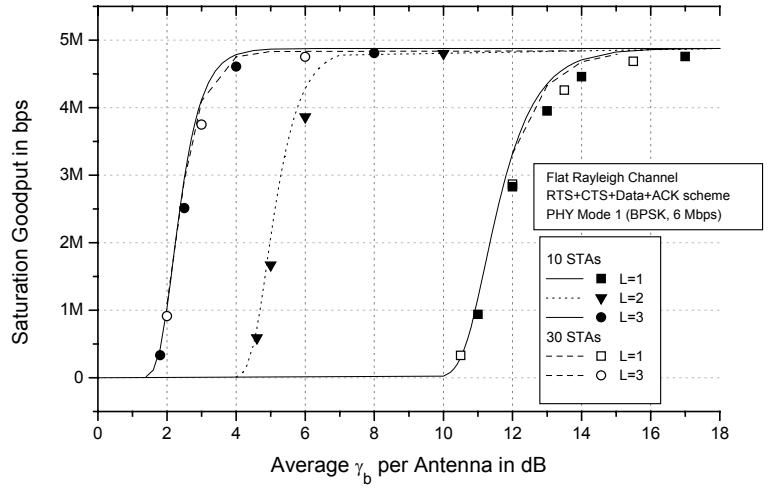

Figure 4. Analytical (straight lines) and simulation (marks) results for the saturation goodput in bps for <u>the PHY mode 1</u> as a function of SINR per bit. Results parameterized by the number of STAs and received antennas.

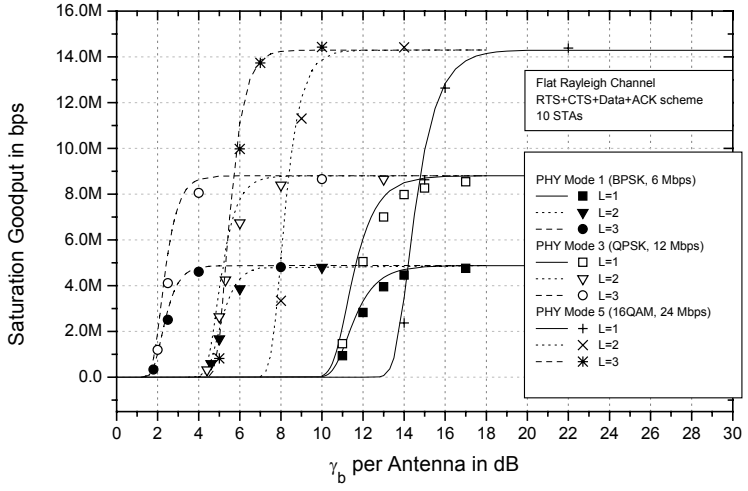

Figure 5. Analytical (straight lines) and simulation (marks) results for the saturation goodput in bps of the <u>mandatory BSS rate</u> as a function of SINR per bit and the number of received antennas.

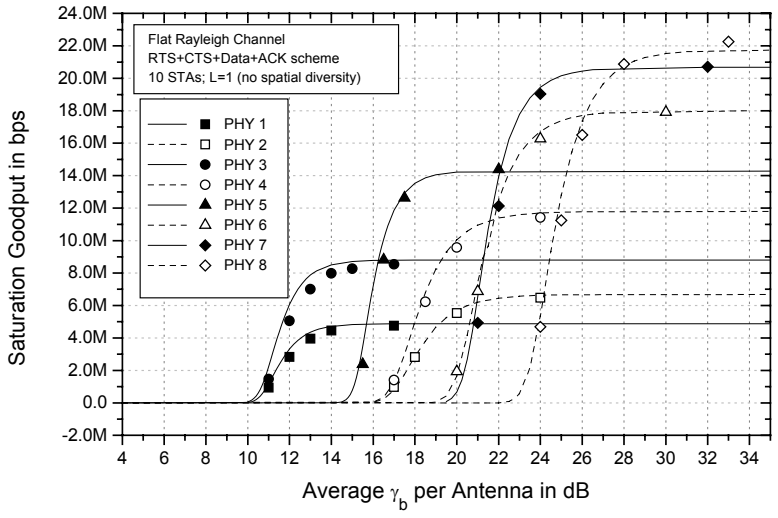

Figure 6a. No spatial diversity (L=1).

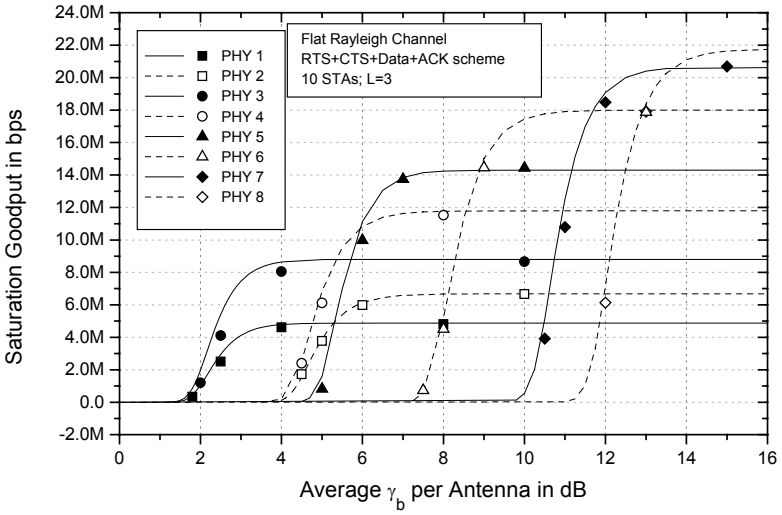

Figure 6b. Spatial diversity with 3 receiving antennas (L=3).

Figure 6. Comparison between analytical (straight lines) and simulation (marks) results for the saturation goodput in bps for all IEEE 802.11a PHY modes as a function of SINR per bit.

5. FINAL REMARKS

In this contribution we have derived and validated a joint MAC and PHY cross-layer goodput saturation model that can be confidentially used to assess the performance of IEEE 802.11a ad hoc networks operating under the RTS/CTS operational mode. We have assumed a flat fading Rayleigh channel that is uncorrelated at symbol level and independent across of the OFDM carriers. In a future work we are going to present the performance of IEEE 802.11a networks

with adaptive link techniques for temporally correlated Nakagami-m fading channel in environments with spatial diversity [HOEFEL 2005]. Based on the interesting remarks of anonymous reviewers, we are developing an analytical data link and physical layer model in order to asses the system performance with a limited number of retransmissions [CHATZMISIOS 2003] for saturated and un-saturated traffic conditions [WU 2002].

6. REFERENCES

Bianchi, G. (2000) "Performance Analysis of the IEEE 802.11 Distributed coordination function," In: IEEE Journal on Selected Areas of Communication, v.18, no. 3, pp. 535-547, March 2000.

Chatzimisios, P. et. al. "IEEE 802.11 packet delay: a finite retry analysis," In: GLOBECOM, pp. 950-954, 2003.

Conan, J. (1984) "The weight spectra of some short low-rate convolutional codes," In: IEEE Trans. Communications**,** vol. 32, pp. 1050-1053, Sept. 1984.

Haccoun, D. and Bégin, G (1989) "High-rate punctured convolutional codes for Viterbi and Sequential decoding", In: *In:* IEEE Trans. Communications**,** vol. 37, n. 11, p. 1113-1120, Nov. 1989.

IEEE 802.11 (1999) "Wireless LAN Medium Access Control (MAC) and Physical Layer (PHY) Specifications, Standard, "IEEE, Aug. 1999.

IEEE 802.11a (1999) *"Part 11: Wireless LAN Medium Access Control (MAC) and Physical Layer (PHY) Specification – Amendment 1: High-speed Physical Layer in the 5 GHz band",* supplemented to IEEE 802.11 standard, Sept. 1999.

Hoefel, R. P. F. and de Almeida, C. (1999) "The performance of CDMA/PRMA for Nakagami-m frequency selective fading channel", In: Electronics Letters, vol. 35, no. 1, 1999, pp 28-29.

Hoefel, R. P. F. and de Almeida, C. (2004) "Performance of IEEE 802.11-based networks with link level adaptation techniques", In: Proceedings of IEEE VTC 2004-Fall, 2004.

Hoefel, R. P. F. (2005) "Cross-Layer Goodput Saturation Traffic Analysis of IEEE 802.11a Networks with Link Level Techniques**",** In: submitted to IEEE VTC 2005-Fall, 2005.

Proakis, J. G. (2001) "*Digital Communications",* New York, 2001.

Puersley, M. B and Taipale, D. J. (1987) "Error Probabilities for Spread-Spectrum Packet Radio with Convolutional Codes and Viterbi Decoding," *In:* IEEE Trans. Communications**,** vol. 35, n. 1, p. 1-12, Jan. 1987.

Qiao, S. D., Choi S. and Shin, K. G. (2002) "Goodput Analyzes and Link Adaptation for the IEEE 802.11a Wireless LANs," In: IEEE Trans. Mobile Comp., pp. 278-292, 2002.

Yang, L. and Hanzo, L. (2000) "A recursive algorithm for the error probability evaluation of M-QAM," In: IEEE Comm. Letters, vol. 4, pp. 304-306, Oct. 2000.

Wu, H.-T et. al. (2002) "Performance of reliable transport protocol over IEEE 802.11 wireless LANs: analysis and performance," In: INFOCOM, pp. 599-607, June 2002.